

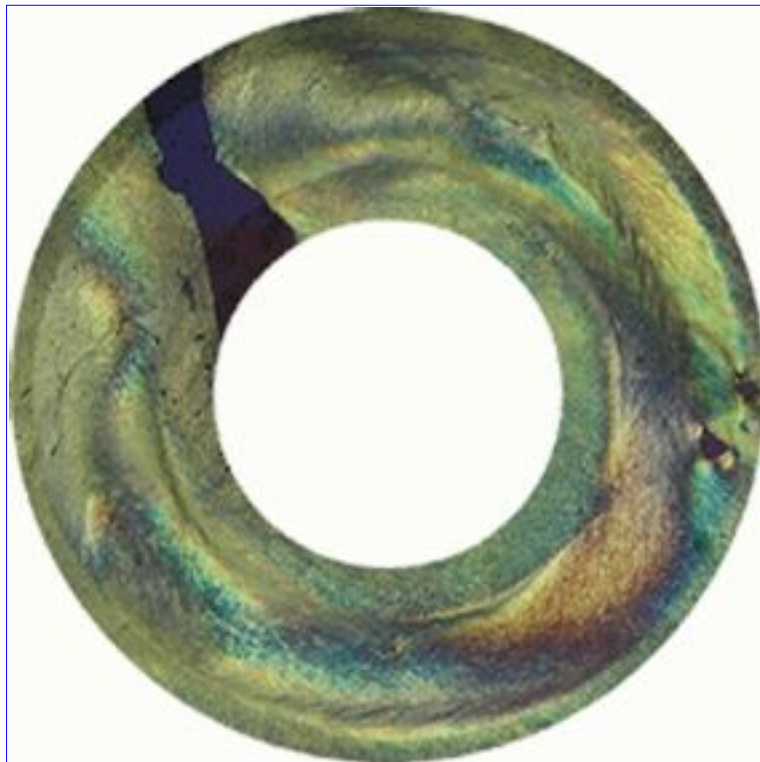


Development of S-C' type cleavage in Paraffin wax using a circular shear rig

M. Hafner , C.W. Passchier

Institut fuer Geowissenschaften der Universitaet Mainz, Abt. Tektonophysik,
Becherweg 21, 55099 Mainz, Germany

Email mhafner@mail.uni-mainz.de
cpasschi@mail.uni-mainz.de



Click in ring to continue

Hafner, M. and Passchier, C.W. 2000. Development of S-C' type cleavage in Paraffin wax using a circular shear rig. In: Stress, Strain and Structure, A volume in honour of W D Means. Eds: M.W. Jessell and J.L.Urai. Volume 2, Journal of the Virtual Explorer. ISSN 1441-8126 (Print). ISSN 1441-8134 (CD-ROM). ISSN 1441-8126 (On-line at www.virtualexplorer.com.au/VEjournal/Volume2).

1 Introduction

The geometry of microstructures is an important source of information on the development of mylonite zones and on the kinematics and dynamics of flow in them. Shear band cleavage is an important as a commonly used shear-sense indicator in mylonites, although its development is incompletely understood. Two types of shear band cleavage are distinguished in the literature: S-C-type and S-C'-type cleavage ([Berthé et al. 1979a, b](#)) ([Figure 1](#)). In our experiment



we focused on the development of S-C' type cleavage ([Figure 2](#)), which is common in micaceous mylonites: S (cleavage)



planes represent a penetratively developed foliation and spaced C'-type shear bands are oblique to shear zone boundaries and to the S-planes ([White 1979b](#), [Platt and Vissers 1980](#)) ([Figure 1](#)). The angle between shear bands and the shear zone margin is 15-35° ([Dennis and Secor 1987](#), [Passchier 1991b](#), [Blenkinsop and Treloar 1995](#)). Normally, only one set of shear bands is developed, with a sense of slip synthetic to the shear-sense of bulk flow. The shear bands may be composed of the same mineralogy as the rest of the rock (e.g. [Gapais and White 1982](#)) or they may show compositional changes typical of retrograde metamorphic reactions (e.g. [McCaig 1987](#), [Norrell et al. 1989](#)) or of the concentration of less soluble material by mass transfer.

S-C'-type shear band cleavage seems to develop late during shear zone activity after a strong mineral preferred orientation has already been established, and probably represents an energetically favourable flow partitioning in strongly anisotropic materials ([Platt and Vissers 1980](#), [Platt 1984](#), [Dennis and Secor 1987](#), [Passchier 1991b](#)). The initiation mechanism of shear bands is related to the amplification of perturbations in the planar anisotropy of a foliated host rock ([Cobbold et al. 1971](#), [Cobbold 1976](#)) and a response to hardening of deforming mylonites (e.g. [White et al. 1980](#), [Passchier 1986](#)). In order to increase understanding of shear band cleavage development, we experimentally modelled the development S-C' type cleavage and the influence of the S-C' cleavage geometry on flow behaviour. We carried out experiments in paraffin wax, an organic material with non-Newtonian rheology in which shear bands can develop. Experiments were carried out in a circular shear rig that has the advantage that very high strain could be obtained. Moreover, the



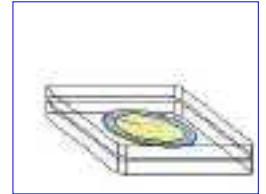
deformation process can be observed and monitored in transmitted light down to the scale of individual grains.



2.1 Apparatus

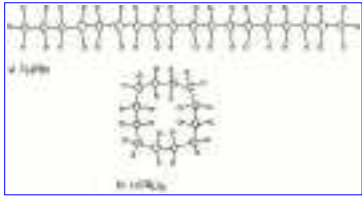


The ring-shear apparatus (Figure 3) used in this experiment can model non-coaxial progressive deformation in paraffin. A disc shaped sample is wedged between two glass plates and is deformed in torsion by rotation of the upper glass plate around a central axis while the lower plate remains fixed (Movie 1). With the help of two frosted grips of different diameter (each etched on to one of the glass slides) an annular shear zone is created. The paraffin is only connected to the glass slides along the frosted grips. Inside the annular shear zone paraffin deforms by a non-coaxial flow with the vorticity vector parallel to the rotation axis of the upper glass slide.



2.2 Experimental Materials

Paraffinic hydrocarbons, or paraffin wax, are straight chained or branched saturated organic compounds with the composition C_nH_{2n+2} (Figure 4). The



purity of paraffin is a question of refining degree. The industrially used paraffin and paraffin candles consists mostly of different molecular structures. The macrocrystalline paraffin wax that we used chiefly consists of saturated, normal C_{18} - C_{30} hydrocarbons and smaller

amounts of iso-alkanes and cycloalkanes with a molecular weight between 250-450. At room temperature the paraffin crystals are needle or plate shaped. A crystallographic change called allotropic transition occurs in an equilibrium transition temperature range below the melting point. The higher temperature phase is characterised by concentration of defects and a molecular structure that can rotate along the long axis (Kwang-Sup 1984). At still higher temperatures, the stable structures are systems of higher symmetry. The crystal structure depends on the molecular composition of paraffin. C_{18} - C_{26} has triclinic crystal symmetry and C_{28} - C_{36} has a monoclinic symmetry. Paraffin wax is usually described by the range of its melt temperature, rather than chain length (e.g. 56°-58°C wax). The rheological behaviour of paraffin wax has been investigated experimentally by several authors (Mancktelow 1988, Cobbold 1975, Neurath & Smith 1982). All investigated types of paraffin wax exhibit a power low creep behaviour over the limited but experimentally relevant temperature range with stress exponents of 2.6 (Cobbold 1975), 1.8 (Neurath & Smith 1982) and 2.4-4.1 (Mancktelow 1988).



2.3 Preparation

The experiment described in this paper was performed with paraffin (melting point range between 56° and 58°C) mixed with a small fraction of 800-grit silicon carbide particles. Silicon carbide grains act as marker particles for flow analysis. Sixty-two milligrams of paraffin (56°C-58°C) with random distributed silicon particles were pressed in a hand-driven pneumatic press for 20 sec at 50 bar and then manually insert between two glass slides with frosted grips. Both glass slides were coated with thin film of a liquid soap to reduce the friction between paraffin and glass slides.



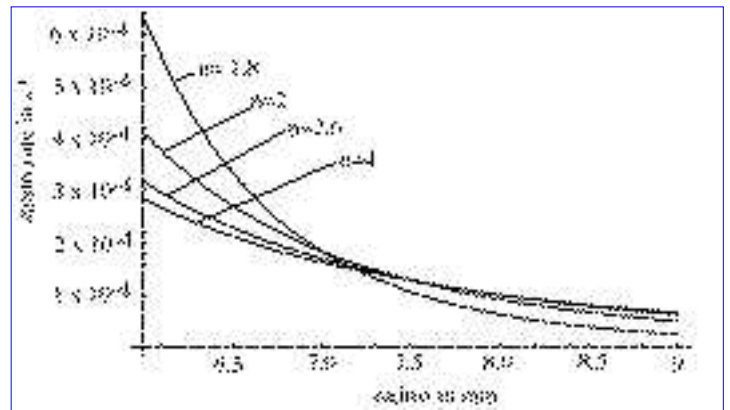
3 Experimental conditions

A small motor was used to rotate the upper glass slide at a constant rate of 0.5 revolutions per hour, which produced a relatively smooth, non-coaxial circular (Figure 5). Couette flow in the paraffin in the annular shear zone. Flow lines



are circular but parallel to the frosted grips and the flow pattern therefore bears a resemblance to that of simple shear: no stretching occurs parallel to the grips. A circle parallel to grips is defined as flow circle, similar to the flow plane of simple shear (Ten Brink & Passchier 1995). The experiment

was conducted at a homologueous temperature (T/T_{melting}) of 0.88. The circular shape of the specimen chamber induces a gradient of increasing flow stress and strain rate over the sample. A gradient in shear strain rate ($\dot{\gamma}$) exists, decreasing in paraffin from inner shear zone boundary to the outer in relation to

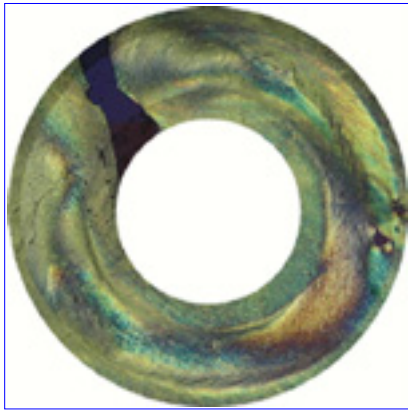


$\left(\frac{1}{r^2}\right)$, where r is the distance from a position in the annular shear zone the rotation axis (Figure 6) (Masuda 1994). The imposed annular shear strain (γ) is calculated as a circular displacement of the outer frosted grip, divided by shear zone width (Passchier & Sokoutis 1993).



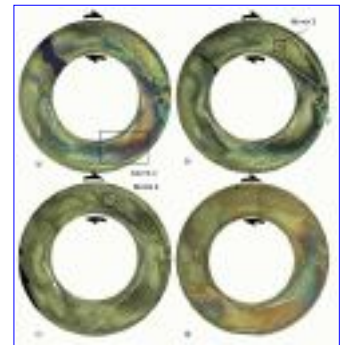
4.1 Deformation of Paraffin wax to an annular shear strain of 1.3

During the experiment a dextral shear sense was imposed on the sample and soon after deformation started, needle shaped paraffin-grains developed a preferred grain shaped orientation (s_1) (Figure 7 or Movie 2).



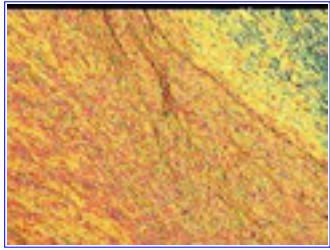
The preferred grain shape orientation relative to the shear zone boundary was not constant. On the left side of movie 2 the grain shape fabric was inclined at a constant angle, while on the right hand side the grains built a concave structure in the annular shear zone. This indicates that deformation on the left hand side includes a shortening component perpendicularly to the shear zone boundary.

Along the inner grip strongly elongated grains are common, oriented oblique to the shear zone boundary. Finite strain was not homogeneously distributed over the sample and increased towards the inner grip. Locally, along the outer grip in a domain (H) with elongated grains, a fabric change is visible (Movie 2) with an indication of dextral shear sense. This domain of higher strain gradually widens during the experiment. A hole on left side of the sample closed during the experiment. (Figure 8)



4.2 Deformation of paraffin wax to a shear strain of 6.0

At a 10x magnification and under cross-polarised light we observed localisation of deformation into shear bands (a, b) with the same shear sense as the imposed bulk shear (Movie [3](#) c' lines). The bands (a, b) are C'-type shear



bands with angles between $25-15^\circ$ to the shear zone boundary, are situated in an area with high concentration of elongated grains, and lie close to a fabric with less deformed grains (Movie [3](#)). Their orientation (a, b) changed gradually,

but in opposite directions during the deformation and both shear bands were stretched. A strong shape fabric formed close to the shear bands (a, b) and this zone widened in the paraffin, whereby the growth of the fabric was fastest in direction parallel to the shear band (a). (Movie [3](#)) shows

the S-C' type cleavage with oblique shear bands (C') and microlithons ([Passchier & Trouw 1996](#)). The microlithons rotated with respect the shear zone boundary, as is clearly visible in (Movie [3](#)).



4.3 Deformation of Paraffin wax to an annular shear strain of 18

At progressive deformation and a magnification of 20x in cross- polarised light

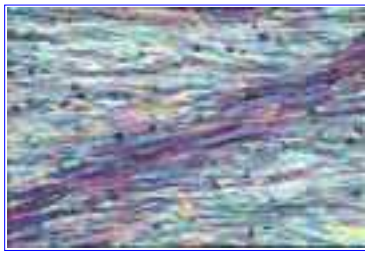


(Movie [4](#)) a S-C' Type cleavage is now well developed with foliated microlithons (M) and C'-shear bands. Strongly elongated grains define the shear bands, which are wavy, anastomosing and short. The shear bands (Movie [4](#)) were not > all active at the same time. First the shear bands 1, 2, 3 were activated and with progressive deformation, the movement around the S-C' cleavage was concentrated along shear band 4. Microlithons have an asymmetric shape and rotated with development of a sigmoidal shape foliation (s) between the shear bands (C'). In the microlithon core the foliation is less intensive as inside the shear bands (C').



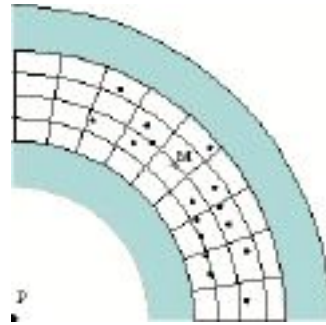
5.1 Methods

Digitalisation of silicon carbide particles at different time intervals (Figure 9)



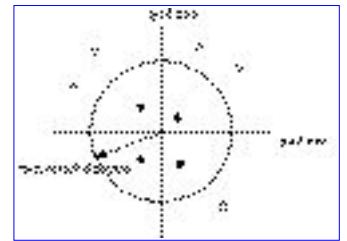
around the S-C' fabric allow us to monitor movement of particles and to calculate the local deformation tensor \mathbf{F} with the program "marker analysis" (Bons et al. 1993).

The program superimposed a regularly spaced polar grid



on the sample.

The grid origin was at the rotation centre of the upper glass slide and a second marker point in the annular shear zone was chosen to fix a second reference axis. The position of each marker point at time (t) is defined by its distance to the origin and its polar angle to the reference particle. The position of each grid node is defined with respect to four adjacent marker particles occupying at least three different quadrants. A deformed polar grid can be constructed with the technique of a least squares best fit method which determine the displacement of each grid node from the displacement of the four adjacent marker particles.

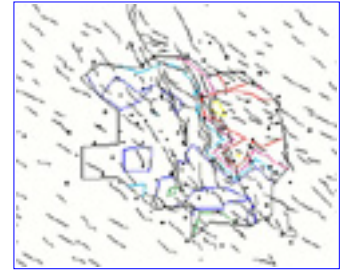


Our experiment is virtually two-dimensional and a deformation tensor \mathbf{F} at any point can be fully described by four independent coefficients, whose values depend on the chosen reference frame. The tensor can be expressed by deformation parameters such as finite strain R_f , a finite 'mean' vorticity number W_n (Passchier 1988) and area change A_f . A_f is 1 for absence of dilation and can represent area decrease or area increase ($A_f > 1$). W_n is a measure of the rotational component of the deformation normalised for strain (Truesdell 1953, Passchier 1988). Positive vorticity numbers indicate a bulk clockwise rotation. W_n is 0 for a pure shear deformation, 1 for a dextral simple shear deformation and $W_n = 1$ indicates a rigid body rotation.



5.2 Contour plots for an annular shear strain of 6.0

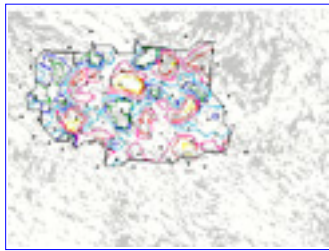
Information about the distribution of vorticity number W_n , area change A_f and strain ration R_f along the S-C fabric is given in (Movie [5](#)). Four pictures were used for analysis of Movie [5](#) are separated by time steps of 22 minutes. 100 markers were digitised for the four pictures. The R_f plots show a dominant value of 1.5 along the S-C' fabric while the surrounding areas were less or not deformed (R_f value close to 1). With time the gradient to the less deformed areas becomes steeper, but the more strained areas widen in the shear band (C') direction. W_n (Movie [6](#)) shows high values around the S-C' fabric, indicating an approach of a super-simple shear ([DePaor 1988](#)) in several directions. On the left hand side of the image are domains with negative W_n . Domains of simple shear ($W_n = 1$) are located within the S-C' cleavage and a pure shear component ($W_n = 0$) is noticeable along the shear band (a). The S-C' fabric is not situated in a simple shear environment.



5.3 Contour plots for an annular shear strain from 13.4 to 18

Thirteen pictures separated by time steps of 3 minutes were used for analysis of movie [4](#)). 100 markers were digitised for the thirteen pictures. The R_f values

increase locally to 1.5 along the shear bands and the microlithons are characterised by unstrained areas, although these areas shrink with the time and the strain gradient increases from the microlithons to the shear bands (C').



On the left side a strain concentration is visible with increasing deformation. The contour plots of W_n show super-simple shear in two directions in the S-C' fabric. At the start of the movie W_n varies along the shear bands. W_n at shear band tips show an anticlockwise rotation and that in the center a clockwise rotation. Values of 1 were localised around the shear bands and with progressive deformation the areas of super-simple shear shrink at the expense of a simple shear.



6 Conclusion

Paraffin wax seems to be a useful analogue material to observe and analyse the development of S-C' Cleavage. In a late stage of deformation of the wax the C'-type shear bands develop in highly anisotropic paraffin characterised by an intensive foliation (s1). Only one set of C'-type shear bands oblique to the shear zone boundary and foliation (s) were developed. Shear bands may denote weak areas or areas of plastic flow. They may be comparable to the development of natural C'-type shear bands in mylonites, which are also short, wavy and anastomosing in a strongly anisotropic material. The development of C'-type shear bands in paraffin are restricted to a $W_n < 1$ or to strain partitioning inside the annular shear zone. The sequence of development and rotation of C'-type shear bands is complicated, a fact that can not be appreciated from the end product as observed in thin section.



7 References

- Berthé, D., Choukroune, P. & Jégouzo, P.** 1979a. Orthogneiss, mylonite and non co-axial deformation of granites: the example of the South Armorican shear zone. *Journal of Structural Geology* 1, 31-42.
- Berthé, J., Choukroune, P. & Gapais, D.** 1979b. Orientation préférentielles du quartz et orthogneissification progressive en régime cisailant: l'exemple du cisaillement sud-Armorcain. *Bulletin de Minéralogie* 102, 265-272.
- Blenkinsop, T. G. & Treloar, P. J.** 1995. Geometry, classification and kinematics of S-C fabrics. *Journal of Structural Geology* 17, 397-408.
- Bons, P. D., Jesell, M. W.** 1993. Manual for the programs "Marker Analysis and Markers
- Bons, P. D., Jesell, M. W. & Passchier, C. W.** 1993. The analysis of progressive deformation in rock analogues. *Journal of Structural Geology* 15(3-5), 403-411.
- Cobbold, P. R., Cosrove, J. W. & Summers, J. M.** 1971. Development of internal structures in deformed anisotropic rocks. *Tectonophysics* 12, 23-53.
- Cobbold, P. R.** 1975. Fold Propagation in single embedded layers. *Tectonophysics* 27, 333-351.
- Cobbold, P. R.** 1976. Mechanical effects of anisotropy during large finite deformations. *Bulletin de la Société géologique de France* 18, 1497-1510.
- DePaor, D. G.** 1994. The role of asymmetry in the formation of structures. *Journal of Structural Geology* 16, 467-475.
- Dennis, A. J. & Secor, D. T.** 1987. A model for the development of crenulations in shear zones with applications from the Southern Appalachian Piedmont. *Journal of Structural Geology* 9, 809-817.
- Gapais, D. & White, S. H.** 1982. Ductile shear bands in a naturally deformed quartzite. *Textures and Microstructures* 5, 1-17.
- Kwang-Sup, L.** 1984. Synthese, Analytik und physikalische Eigenschaften linearer und cyclischer Paraffine mit mehr als 20 Kettenglieder. Unpubilshed

Ph.D. thesis, Freiburg.

Mancktelow, N. S. 1988. The rheology of paraffin wax and its usefulness as an analogue for rocks. *Bulletin of the Geological Institutions of the University of Uppsala* 14, 181-193.

Masuda, T., Mizuno, N., Kobayashi, M. & T. G. N. & Ozoh, S. 1994. Stress and Strain estimates for Newtonian and non-Newtonian materials in a rotation shear zone. *Journal of Structural Geology* 31, Short Note for *Journal of Structural Geology*.

McCaig, A. M. 1987. Deformation and fluid-rock interaction in metasomatic dilatant shear bands. *Tectonophysics* 135, 121-132.

Neurath, C. & Smith, R. B. 1982. The effect of material properties on growth rates of folding and boudinage: experiments with wax models. *Journal of Structural Geology* 4(2), 215-229.

Norrell, T. G., Teixell, A. & Harper, G. D. 1989. Microstructure of serpentinite mylonites from the Josephine ophiolite and serpentinitization in retrogressive shearzones, California. *Geological Society of America Bulletin* 101, 673-682.

Passchier, C. W. & Simpson, C. 1986. Porphyroclast systems as kinematic indicators. *Journal of Structural Geology* 8(8), 831-843.

Passchier, C. W. 1988. Analysis of deformation paths in shear zones. *Geologische Rundschau* 77, 309-318.

Passchier, C. W. 1991b. Geometric constraints on the development of shear bands in rocks. *Geologie en Mijnbouw* 70, 203-211.

Passchier, C. W. & Sokoutis, D. 1993. Experimental modelling of mantled porphyroclasts. *Journal of Structural Geology* 15(7), 895-909.

Passchier, C. W. & Trouw, R. A. J. 1996. *Microtectonics*. Springer, Heidelberg.

Platt, J. P. & Vissers, R. L. M. 1980. Extensional structures in anisotropic rocks. *Journal of Structural Geology* 2, 397-410.

Platt, J. P. 1984. Secondary cleavages in ductile shear zones. *Journal of*

Structural Geology 6, 439-442.

Ten Brink, C. E. & Passchier, C. W. 1995. Modelling of mantled porphyroclasts using rock analogue materials. *Journal of Structural Geology* 17, 131-146.

Truesdell, C. 1953. Two measures of vorticity. *J. Rational Mech. Anal.* 2, 173-217.

White, S. H. 1979. Large strain deformation: report on a Tectonic Studies Group discussion meeting held at Imperial College, London. *Journal of Structural Geology* 1, 333-339.

White, S. H., Burrows, S. E., Carreras, J., Shaw, N. W. & Humphreys, F. J. 1980. On mylonites in ductile shear zones. *Journal of Structural Geology* 2, 175-187.

Figure 1



5 cm

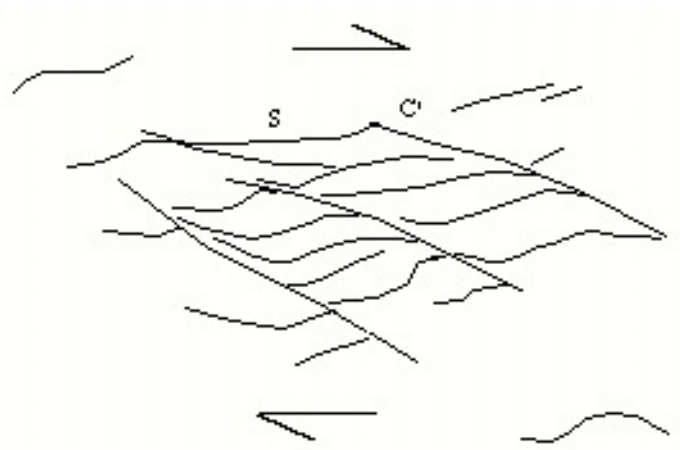
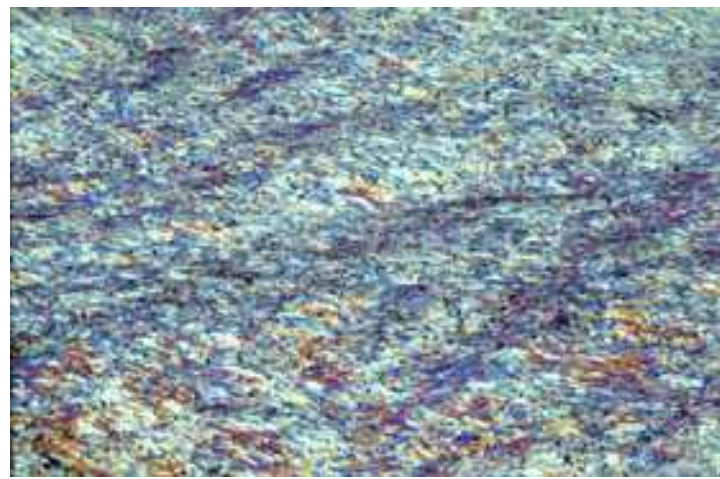


Figure 1

S-C'-Type cleavage from the helvetic naps





0.25 mm

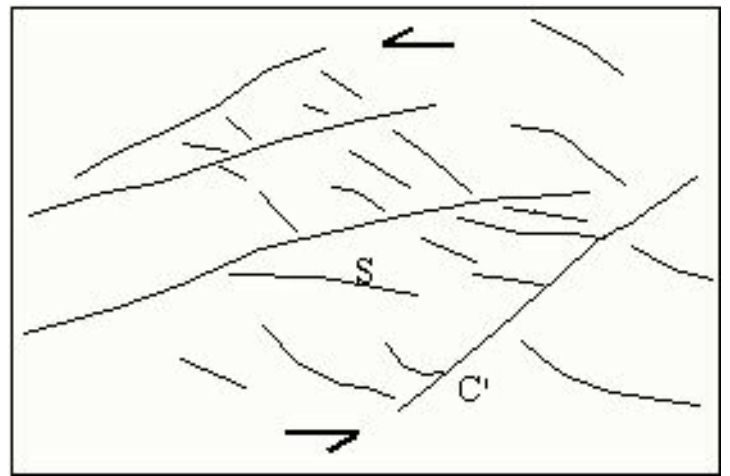


Figure 2

S-C'-Type cleavage in paraffin wax
(56°-58°C) at a temperature of 50°C and
a strain rate (γ) of 6.2






Figure 3

Torsion rig

Torsion rig for modeling a non-coaxial progressive deformation at constant temperature and strain rate





1.0 cm

Movie 1

Squetch of torsion rig

A disc shaped sample is wedged between two glass plates and is deformed in torsion by rotation of the upper glass plate around a central axis, while the lower plate remains fixed. The velocities (v_I , v , v_O) of particles inside the sample are different and depending on the locality inside the annular shear zone.

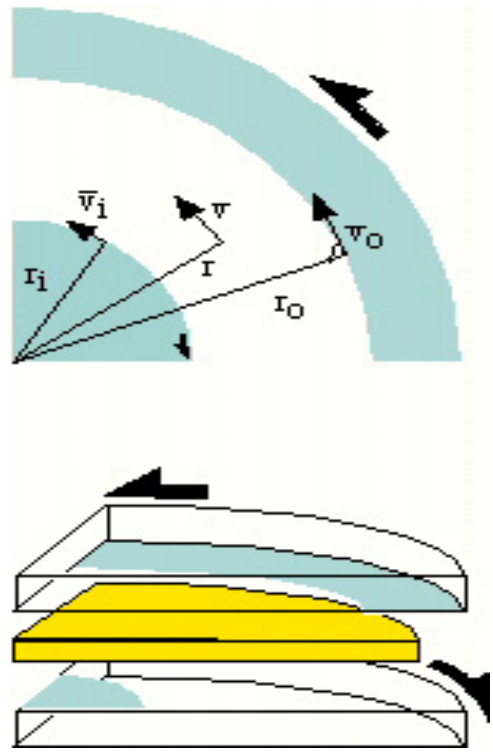
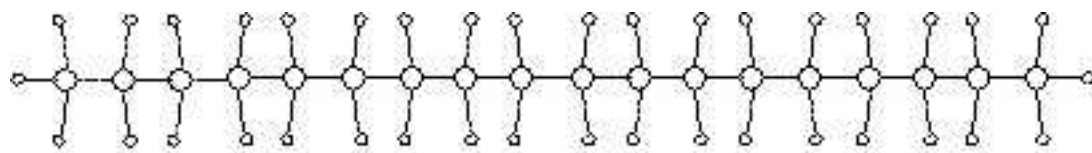
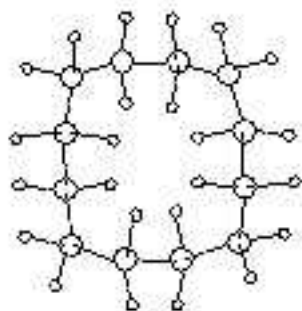


Figure 4



a) $C_{18}H_{38}$



b) C_6H_{12}

Figure 4

Structure of paraffin wax

Macrocrystalline paraffin wax are mixtures, which consist chiefly of saturated, normal C_{18} - C_{30}

hydrocarbons (a) and smaller amount of iso-alkanes and cycloalkanes (b).



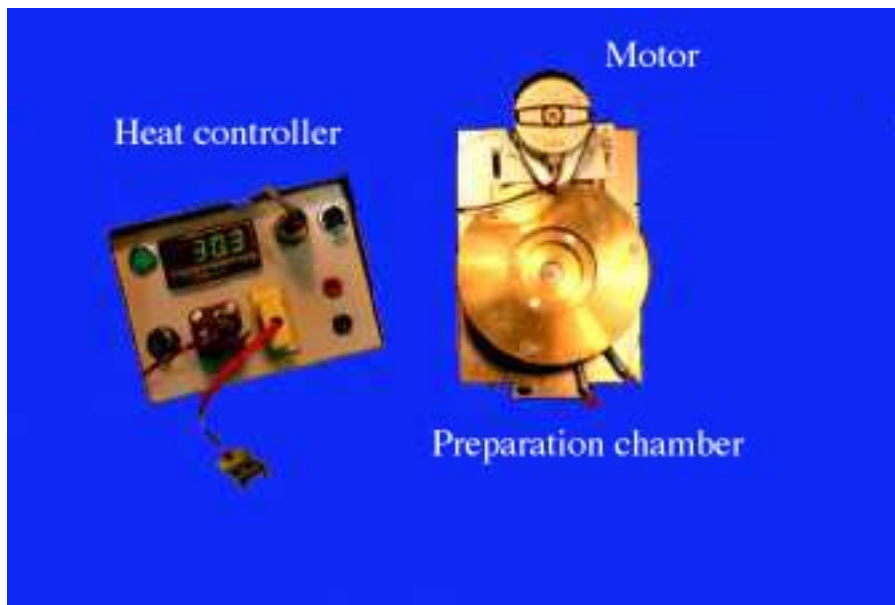


Figure 5

Torsion rig

A small motor was used to rotate the upper glass slide at a constant rate of 0.5 revolutions per hour, which produced a relatively smooth, non-coaxial circular Couette flow in the annular shear zone. The temperature was hold constant with a heat controller



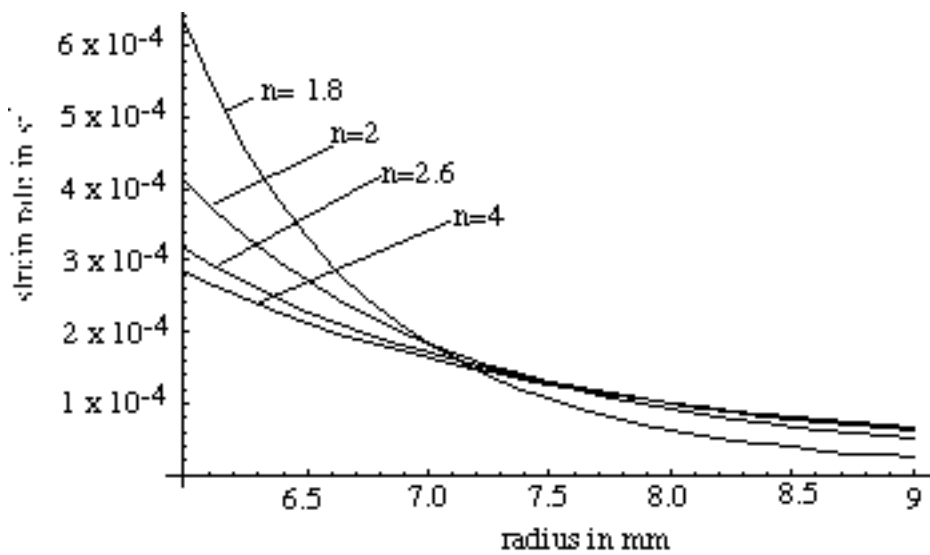


Figure 6

Diagram for strain rate variation of paraffin wax with different stress exponents in a circular rig with an outer diameter of 24 mm for the smaller frosted grip and an inner diameter of 36 mm for the outer frosted grip. All investigated types of paraffin wax exhibit a power law creep behaviour over the limited but experimentally relevant temperature range with stress exponents of 2.6 (Cobbold 1975), 1.8 (Neurath & Smith 1982) and 2.4-4.1 (Mancktelow 1988).



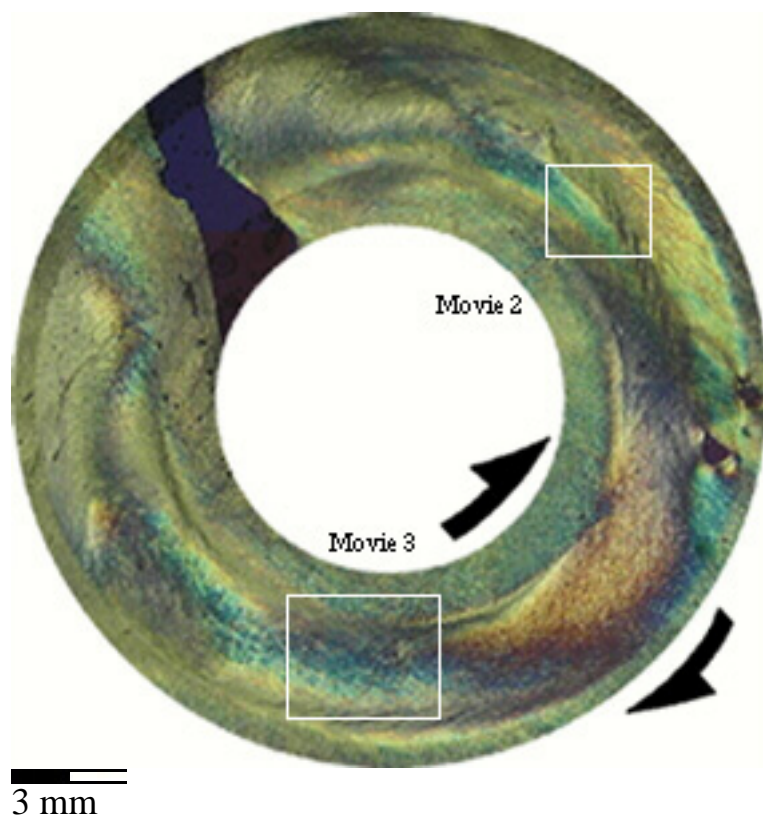


Figure 7

Photomicrographic under crossed nicols of the entire annular shear zone at beginning of deformation. The position of movies 2 and 3 is shown





1.0 mm

Movie 2

Deformation of paraffin wax to an annular shear strain of 1.4 rad /cm at outer shear zone boundary

During a dextral shear strain an oblique preferred grain shape orientation (s_1) was build and locally along the shear zone boundaries domains of high strain (H). Left picture shows the situation at the beginning of deformation. The movie consists of picture with laps of 450s



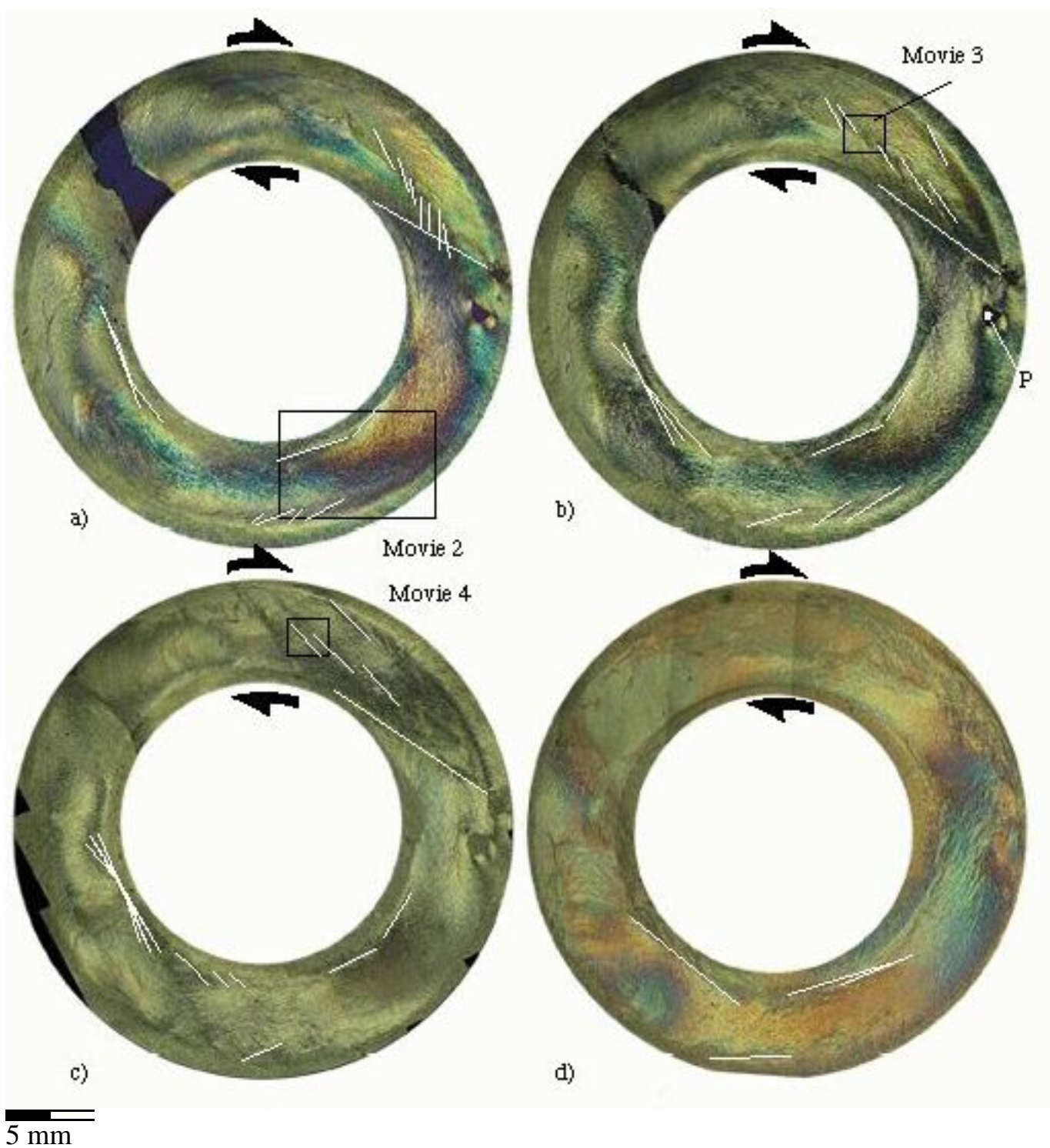
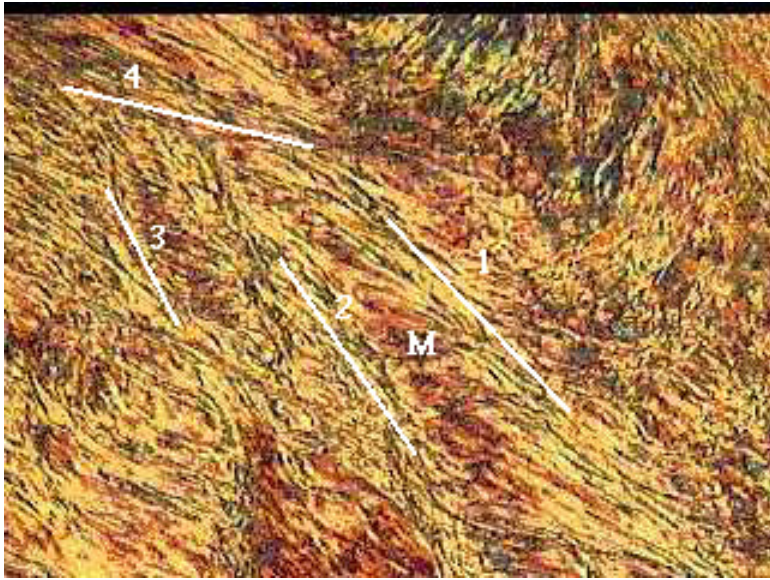


Figure 8

Photomicrographic under crossed nicols of the entire annular shear zone at different finite strains. The place of the movie 2, 3 and 4 are signed. Figure a-d show the development of microstructures in the entire sample. The finite strain was outer shear zone boundary at a 1.3, at b 6.0 at c 8.4 and at d 18.3. The white lines indicate some shear bands (c') and thrust in the experiment. All four pictures were rotated relative to the fix point P.



0.1 mm

Movie 4

Deformation of paraffin wax to an annular shear strain of 18.0 rad /cm at outer shear zone boundary

At a 20x magnification and under cross-polarised light we observed a well developed S-C' Type cleavage with foliated microlithons (M) and C'-shear bands (1, 2, 3, 4).

Strongly elongated grains define the shear bands, which are wavy, anastomosing and short. Pictures are taken with time laps of 450s



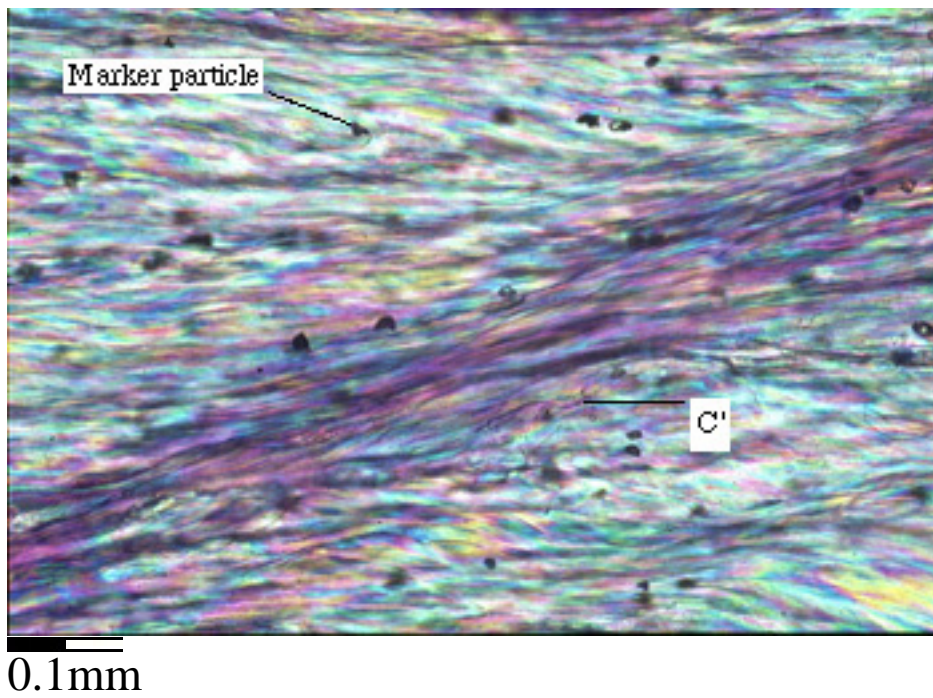


Figure 9

S-C'-type shear band with markers
A C'-type shear band in paraffin wax
surrounded by silicon carbide particles. The
rotation of the foliation to the shear band is
clearly visible.



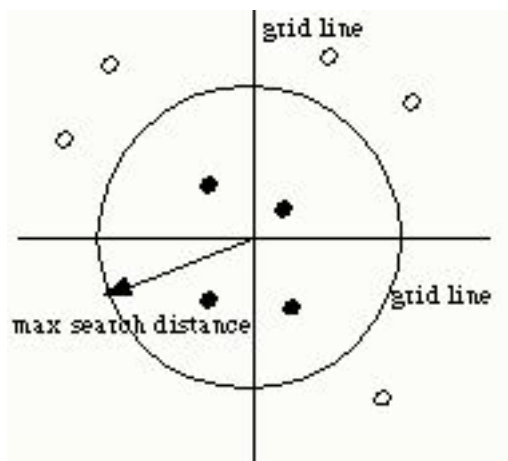


Figure 10

Example of how the marker algorithm works to select markers around a grid node. Select markers are shown in black, other in white. The minimum number of markers is set 4 (Bons & Jessell 1993)



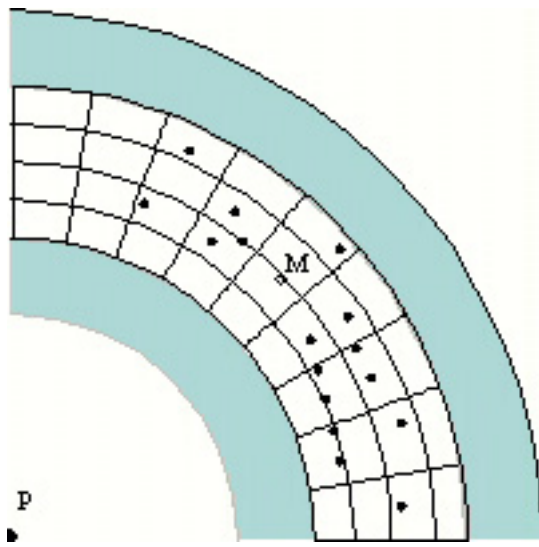


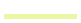





Figure 11

Polar grid between frosted grips with the origin of polar grid at point P. The grid origin was at the rotation centre of the upper glass slide and a second marker point (M) in the annular shear zone was chosen to fix a second reference axis



Movie 5

Strain ration R_f Strain ration R_f distribution

-  1
-  1.1
-  1.2
-  1.3
-  1.4
-  1.5

A shear strain of 2.9 was imposed on the sample along the outer shear zone boundary. Four pictures were used for analysis of [Movie5](#) separated by time steps of 22 minutes. 100 markers were digitised for the four pictures.

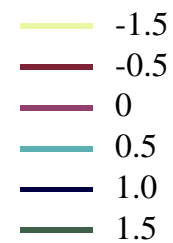




0.25 mm

Movie 6

Vorticity Wn Vorticity distribution



A shear strain of 2.9 was imposed on the sample along the outer shear zone boundary. Four pictures were used for analysis of [Movie5](#) separated by time steps of 22 minutes. 100 markers were digitised for the four pictures.

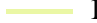






Movie 7

Strain ration R_f Strain ration R_f distribution

Deformation of paraffin wax to an annular shear strain of 18.0 rad /cm at outer shear zone boundary

At a 20x magnification and under cross-polarised light we observed a well developed S-C' Type cleavage with foliated microlithons. Thirteen pictures separated by time steps of 4 minutes were used for analysing the movement of 100 markers and the strain ratio distribution (R_f) (Movie 4). The R_f distribution reflects the S-C'type cleavage in paraffin wax.

-  1
-  1.1
-  1.2
-  1.3
-  1.4
-  1.5



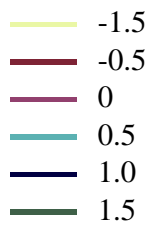
Movie 8

Vorticity W_n Vorticity distribution

Deformation of paraffin wax to an annular shear strain of 18.0 rad /cm at outer shear zone boundary

At a 20x magnification and under cross-polarised light we observed a well developed S-C' Type cleavage with foliated microlithons. Thirteen pictures separated by time steps of 4 minutes were used for analysing the movement of 100

markers and the vorticity distribution W_n (Movie [4](#)). The contour plots of W_n show super-simple shear in two directions in the S-C' fabric.





0.25 mm

Movie 3

Deformation of paraffin wax to an annular shear strain of 6.0 rad /cm at outer shear zone boundary

At a 10x magnification and under cross-polarised light we observed localisation of deformation into shear bands (a, b) with the same shear sense as the imposed bulk shear. Left picture shows the situation at shear strain rate of 2.9 at outer shear zone boundary. The movie shows the S-C' type cleavage with oblique shear bands (C') and microlithons (Passchier & Trouw 1996). The microlithons rotated with respect the shear zone boundary, as is clearly visible. The movie consists of picture with laps of 320s

